Journal of The Electrochemical Society, **162** (4) H1-H7 (2015)
0013-4651/2015/162(4)/H1/7/$33.00 © The Electrochemical Society

Photoelectrochemical Hydrogen Production Using SiC-TiO_2-Sm_2O_3 as Electrode

Isaías Juárez-Ramírez,[z] Leticia M. Torres-Martínez, Christian Gómez-Solís, and Juan C. Ballesteros

Universidad Autónoma de Nuevo León (UANL), Facultad de Ingeniería Civil, Departamento de Ecomateriales y Energía, Ciudad Universitaria, San Nicolás de los Garza, Nuevo León C.P. 66455, México

This paper shows the importance of the synergy effect of SiC-TiO_2-Sm_2O_3 in order to enhance the efficiency of the charge separation in the hydrogen generation by means of photoelectrochemical process. In this work it is reported the photoelectrochemical hydrogen production from an aqueous solution of sulfuric acid using SiC-TiO_2-Sm_2O_3 as photoelectrode. The SiC-TiO_2-Sm_2O_3 was prepared by sol-gel method and thermal treated at 600°C with different content of samarium. The physicochemical characteristics of the as-prepared SiC-TiO_2-Sm_2O_3 powders were measured by scanning electron microscopy (SEM) coupled with energy dispersive spectroscopy (EDS) analysis, Fourier transform infrared spectroscopy (FTIR), ultraviolet-visible absorption spectroscopy (UV-Vis), Photoluminescence analysis (PL), specific BET surface area analysis (S_{BET}) and X-ray diffraction (XRD). Hydrogen was generated on SiC-TiO_2-Sm_2O_3 from a sulfuric acid solution by applying a bias potential under UV light irradiation. The produced photocurrent intensities associated with the hydrogen production after 1800 seconds of reaction depended on Sm_2O_3 concentration, and it was found that hydrogen production increased as Sm^{3+} concentration increases, up to about 2.0 wt%, and then decreased. Finally, the percentage of incident photon conversion efficiency (% IPCE) was determined as a function of Sm_2O_3 concentration and the results showed a maximum value (% IPCE = 4.7) for the sample with 2.0 wt% of Sm^{3+} ions.

Manuscript submitted December 8, 2014; revised manuscript received February 3, 2015. Published 00 0, 2015.

At present, it is necessary to use alternative energy sources to cover the energy demand by population because fossil fuels are diminishing every day. During the last two decades, hydrogen has attracted much attention due to its chemical properties, and it is considered an alternative fuel instead of fossil sources. This is because hydrogen is a regenerative and environmentally friendly fuel with high calorific value, which makes it possible to convert chemical energy to electric energy from a clean energy source with significant production in the future.[1–3] Hydrogen is obtained mainly from water and hydrocarbons, by different processes such as biological,[4] steam or partial oxidation reforming of natural gas,[5,6] water–gas shift reaction,[6] biomass reforming,[7,8] and water photocatalysis.[9] Approximately 95% of hydrogen is generated by steam/partial oxidation reforming, because it is a mature, efficient and cheap technology.[6] The main inconvenient of these technologies is that hydrogen is obtained from fossil fuels, which means that environmental pollution cannot be avoided. On the contrary, water photocatalysis is an interesting advanced chemical technology, but it is still under development because its industrial application is limited to the use of solar energy efficiently.[9]

From the first report of Fujishima and Honda[10] in 1972 about the photoelectrochemical hydrogen production using TiO_2 as photoanode, other investigations on photoelectrochemical hydrogen production have been reported.[11–14] The photoelectrochemical water splitting reaction represents a great challenge because the hydrogen production efficiencies of known catalysts still are too low to meet commercial demands.[15] TiO_2 is a photoanode with high chemical stability, nevertheless only the UV part of the solar spectrum is effective for its application in water splitting due to its large bandgap (3.2 eV). Additionally, the photocatalytic activity of TiO_2 itself is also limited because of the rapid electron/hole pair recombination rate. Promising results based on the chemical modification of TiO_2 indicate that loading the TiO_2 surface with noble metals or noble metal oxides creates electron sinks and holes that enhance the hydrogen production activity.[15–20] In 1998 Ashokkumar[21] reported an overview on semiconductor materials for hydrogen generation, in where silicon carbide (SiC) appears as a strong candidate due to its chemical, optical and mechanical properties. However, few papers[11,22–25] have been found in literature demonstrating the use of SiC as photocathode for water splitting reaction. In fact, SiC has been also reported for hydrogen generation in an electrochemical system without any external voltage for its operation.[11]

On the other hand, the SiC-TiO_2 mixture has been employed as photocatalyst in the redox reactions for acetaldehyde production, 2-propanol degradation, methylacetone oxidation and organic dye degradation.[26–30] Among the studies on the SiC-TiO_2 system found in the literature,[15,31–35] results show that the photocatalytic activity for water splitting and degradation of organic compounds is significantly enhanced due to the synergetic effect between SiC and TiO_2. Also, the presence of metals or metal oxides forming a ternary system, such as Cr_2O_3-SiC-TiO_2, WO_3-SiC-TiO_2, Fe-SiC-TiO_2, Pt-SiC-TiO_2, improves the water splitting activity. Additionally, the incorporation of rare earths (RE) in semiconductor materials have attracted considerable attention due to the modification of the optical, magnetic and electrical properties.[36–41] The presence of RE confers luminescence properties to the semiconductor material, such as low photobleaching, narrow emission bands and larger luminescent lifetimes, which contributes to the increment of the photocatalytic activity.[42–45] Particularly, Li et al.[44] have explored the TiO_2:Sm^{3+} system with different Sm^{3+} concentrations (0–2.0 wt%) and they found that degradation of RhB is improved when Sm^{3+} ion is incorporated. In addition, these authors have reported the existence of a critical concentration of samarium where the efficiency starts to decrease.

It is well known that the electron-hole pair photogeneration is very important for the redox reaction in the photocatalytic process. While in the photoelectrochemical hydrogen production the key factor is the lifetime of photogenerated electrons for the direct reduction of H^+.

Therefore, based on the above mentioned about the ternary compounds and the luminescent properties of the semiconductor materials in the presence of samarium, in this work, a novel ternary composite, SiC-TiO_2-Sm_2O_3, was synthesized by sol-gel method and a subsequent thermal treatment. This material was characterized by several analytical techniques and applied as an electrode in the photoelectrochemical and electrochemical production of hydrogen.

Experimental

SiC-TiO_2 and SiC-TiO_2-Sm_2O_3 electrodes preparation.— SiC-TiO_2 was prepared via sol-gel method from silicon carbide (SiC) commercial powder (mesh 200–450, Aldrich), and titanium (IV) isopropoxide (Aldrich 99.99%) as raw materials. The preparation was as follows: SiC powder was dispersed in 30 mL of ethanol and then was sonicated for 15 minutes; this solution was placed in a reflux system at 70°C and then the titanium isopropoxide was added slowly (1 drop/min) to obtain a gel, which was dried below 100°C. Finally, this material was thermally treated at 600°C for 2 h.[29]

[z]E-mail: isajua13@yahoo.com

For the preparation of SiC-TiO_2-Sm_2O_3 material, similar procedure was used as above described. In this case the samarium was incorporated from 0.5 M samarium nitrate aqueous solution, which is a similar procedure, reported in the literature.[44,45] During the process of formation of SiC-TiO_2-Sm_2O_3, the aqueous solution containing Sm^{3+} ions was added and kept in agitation with the other two components to obtain a homogeneous solution. The water/acetic acid (55 wt% ratio) was added to promote the hydrolysis-condensation process. The formed gel was dried below 80°C for 5 h and the powder was thermally treated at 600°C for 2 h. Finally, this procedure was repeated to obtain SiC-TiO_2-Sm_2O_3 powder at different samarium oxide concentrations (1.0 wt%, 2.0 wt%, 5.0 wt% and 10 wt%).

Each SiC-TiO_2-Sm_2O_3 material was applied onto a copper metallic substrate (1.5 cm × 1 cm) with the finality to obtain the electrode. As metallic substrate was used a conductive copper material with single sided adhesive. Additional experiments by infrared spectroscopy were carried out to observe the chemical stability of this tape (3 M Company) in a 0.5 M H_2SO_4 solution. Each one of the samples was used as working electrode in the electrochemical cell. The amount of powder on the metallic substrate was 1.2 ± 0.1 mg.

Physicochemical characterization.— The phase composition of the SiC-TiO_2 and SiC-TiO_2-Sm_2O_3 powders were examined by X-ray diffraction (XRD) technique using a Bruker AXS D8 Advance instrument with Cu Kα irradiation. The diffraction patterns were collected from 20° to 80°. Scanning electron microscopy (SEM) was carried out on a JEOL JSM-6490LV electron microscope coupled with energy dispersive X-ray spectroscopy (EDS) analysis. The energy bandgap (E_g) was determined by the Kubelka-Munk function using a UV–vis spectrophotometer (Lambda 35 Perkin Elmer Corporation) coupled with an integrating sphere. The room temperature photoluminescence (PL) spectra of the materials were obtained from a Cary Eclipse Fluorescence spectrophotometer (Agilent Technologies) with an excitation wavelength of 370 nm. Specific surface area (S_{BET}) was measured by N_2 physisorption through the BET method using Quantachrome NOVA 2000e equipment. The chemical stability of the metallic substrate was analyzed by infrared spectroscopy from Nicolet 380 FTIR Spectrometer.

Photoelectrochemical (PEC) hydrogen generation.— The experiments were carried out in a conventional three-electrode electrochemical cell (quartz) with a Pt counter electrode and an Ag/AgCl (saturated KCl) as reference electrode. The potential and current were controlled by a potentiostat/galvanostat AUTOLAB PGSTAT302N connected to a personal computer running the system software (NOVA) for data acquisition. The used volume and chemical composition of this electrolytic solution were 100 mL and 0.5 M H_2SO_4, respectively. The electrolyte was prepared using analytic grade reagents (Aldrich) with ultra-pure water and it was deoxygenated by bubbling N_2 for 20 min before each experiment. The hydrogen evolution reaction was monitored by linear voltammetry and chronoamperometry techniques. The PEC experiments were conducted under UV-light illumination using a Hg Pen Ray Light Lamp UVP ($\lambda = 365$ nm, $I_0 = 0.15$ mWcm^{-2}).

Results and Discussion

Structural, morphological, chemical and optical characterization of SiC-TiO_2-Sm_2O_3.— Figure 1 shows the XRD patterns of (a) SiC-TiO_2, (b) SiC-TiO_2-Sm_2O_3 with 10 wt% of samarium content and (c) Sm_2O_3, which were synthesized by sol-gel method and subsequent thermal treatment. According to XRD results, the diffraction peaks in Figure 1a correspond to the pure anatase phase TiO_2 [JCPDS 01-089-4921] and SiC [JCPDS 00-004-0756] and no additional peaks were detected. Likewise, XRD characteristic peaks of TiO_2, SiC and Sm_2O_3 are clearly observed in the Figure 1b and no additional diffraction peaks were detected, which suggest no chemical reaction between SiC-TiO_2-Sm_2O_3 is occurring. Figure 1c shows the diffraction peaks corresponding to the samarium oxide, Sm_2O_3 [JCPDS 00-015-0813]. It is important to mention that diffraction peaks (not showed here)

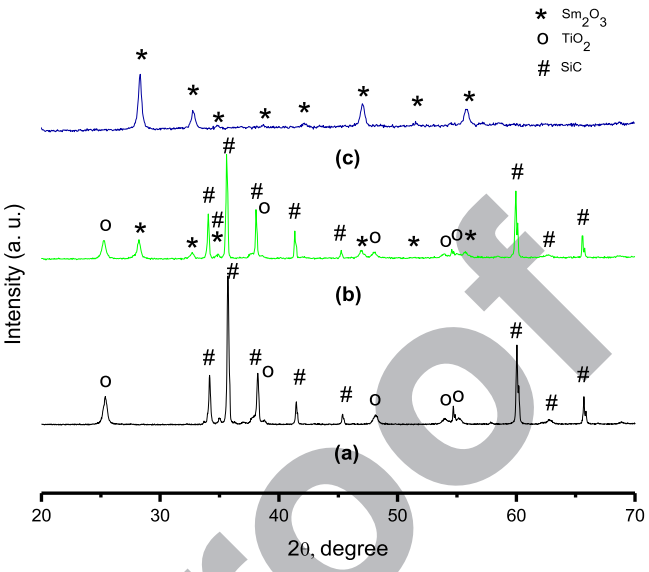

Figure 1. XRD patterns of a) SiC-TiO_2, b) SiC-TiO_2-Sm_2O_3 with 10 wt% and c) Sm_2O_3.

associated with Sm_2O_3 were no detected in the samples when Sm^{3+} ions content was below 10 wt%.

FTIR spectra of (a) SiC-TiO_2 and (b) SiC-TiO_2-Sm_2O_3 with 2.0 wt% and (c) SiC-TiO_2-Sm_2O_3 with 10 wt% is presented in Figure 2. The absorption band at about 1000 and 1200 cm^{-1} corresponds to the stretching vibration of Si-C. Moreover, the characteristic bands at ca. 454 cm^{-1} and 613 cm^{-1} correspond to the Ti-O-Ti and Ti-O vibrations.[46,47] In general, the absorption bands become less intense when the concentration of Sm^{3+} ions increases. This behavior can be attributed to the amount of samarium on SiC-TiO_2, which blocked the surface of this compound.

The SEM images and the corresponding EDS analysis of the SiC-TiO_2-Sm_2O_3 powders with different content of samarium were obtained. The microstructure of all samples is almost similar and consists of several small aggregates on big particles. In order to know the Sm^{3+} contents in the SiC-TiO_2-Sm_2O_3 powders, EDS analysis was conducted and the results are shown in Table I. It is appreciated a good correlation between the real and theoretical composition.

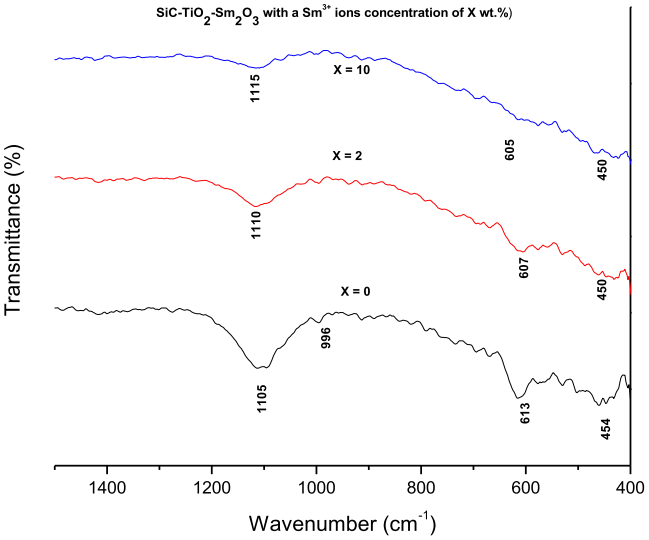

Figure 2. FTIR spectra of (a) SiC-TiO_2 and (b) SiC-TiO_2-Sm_2O_3 with 2.0 wt% and (c) SiC-TiO_2-Sm_2O_3 with 10 wt%.

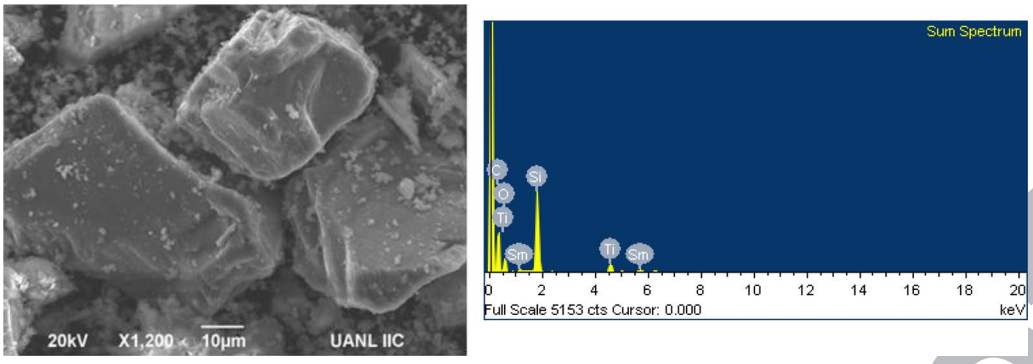

Figure 3. SEM images and its corresponding EDS analysis of the SiC-TiO_2-Sm_2O_3 powders with 2.0 wt% Sm^{3+} ions concentration.

A representative SEM image and EDS spectra corresponding to the SiC-TiO_2-Sm_2O_3 sample containing 2.0 wt% of Sm^{3+} ions is shown in Figure 3.

The specific BET surface area for the prepared SiC-TiO_2 and SiC-TiO_2-Sm_2O_3 powders are also showed in Table I. The obtained values indicated that the specific surface area is directly proportional to the Sm^{3+} ion concentration.

Band gap energy (E_g) was calculated using Kubelka-Munk function from the absorbance spectra showed in Figure 4. It can be observed that all materials (SiC-TiO_2-Sm_2O_3 with different content of Sm^{3+} ions) absorb energy efficiently below ca. 410 nm. As seen in Table I, the bandgap energy values for the synthesized samples containing samarium were around 3.0 ± 0.1 eV, which is very similar to the bandgap energy of SiC-TiO_2 (3.0 eV). In the case of pure Sm_2O_3, its E_g value is around 4.6 eV.

The Figure 5 shows the emission spectra of SiC-TiO_2 and SiC-TiO_2-Sm_2O_3 powders with different Sm^{3+} ions concentration excited at 370 nm. Results indicate that no emission peaks were observed for SiC-TiO_2 sample. It can be seen that each emission spectrum consists of the three peaks at 583, 613 and 664 nm, which correspond to the $^4G_{5/2} \rightarrow {}^6H_{5/2}$, $^4G_{5/2} \rightarrow {}^6H_{7/2}$, and $^4G_{5/2} \rightarrow {}^6H_{9/2}$ transitions, respectively. The luminescence was dominated by the $^4G_{5/2} \rightarrow {}^6H_{7/2}$ transition. It was detected that when Sm^{3+} concentration is 2.0 wt% there is a maximum in the emission intensity of the peaks in each spectrum, then above this concentration the emission intensity decreases as the amount of Sm^{3+} ions in SiC-TiO_2-Sm_2O_3 increases.

Electrochemical and photoelectrochemical characterization of SiC-TiO_2-Sm_2O_3 electrodes.— Linear voltammetry study was performed in the potential range from −0.7 to −0.2 V onto SiC-TiO_2 and SiC-TiO_2-Sm_2O_3 electrodes using a 0.5 M H_2SO_4 aqueous solution; the potential scan was initiated in the negative direction from the open circuit potential (E_{OCP}) at scan rate (υ) of 10 mV s^{-1}.

Electrochemical characterization of the adhesive copper tape.—With the purpose to know the chemical stability of the adhesive copper tape (ACT) used as substrate, an electrochemical study by linear voltammetry was done before testing the materials. Figure 6 shows the linear voltammograms obtained on ACT (used as working electrode) in the acidic solution under dark and UV-light irradiation. It is worth noting

Table I. Specific surface area (S_{BET}), samarium content and energy bandgap (E_g) of SiC-TiO_2-Sm_2O_3.

Sample	S_{BET} (m^2 g^{-1})	Sm^{3+} ions content	E_g (eV)
SiC-TiO_2	39	-	2.9
SiC-TiO_2-Sm_2O_3 (1.0 wt%)	76	0.7	3.1
SiC-TiO_2-Sm_2O_3 (2.0 wt%)	80	1.8	3.1
SiC-TiO_2-Sm_2O_3 (5.0 wt%)	98	5.4	2.9
SiC-TiO_2-Sm_2O_3 (10 wt%)	117	10.2	2.9

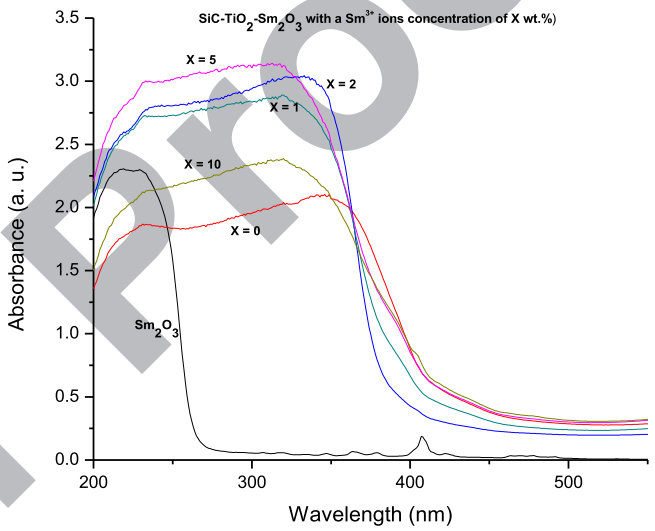

Figure 4. UV-vis spectra of (a) SiC-TiO_2 and (b) SiC-TiO_2-Sm_2O_3 with different concentration of Sm^{3+} ions.

a similar E_{OCP} value, which is approximately −0.34 V in both cases. Also an increase in the magnitude of the cathodic current when the ACT was exposed to the light is clearly appreciated.

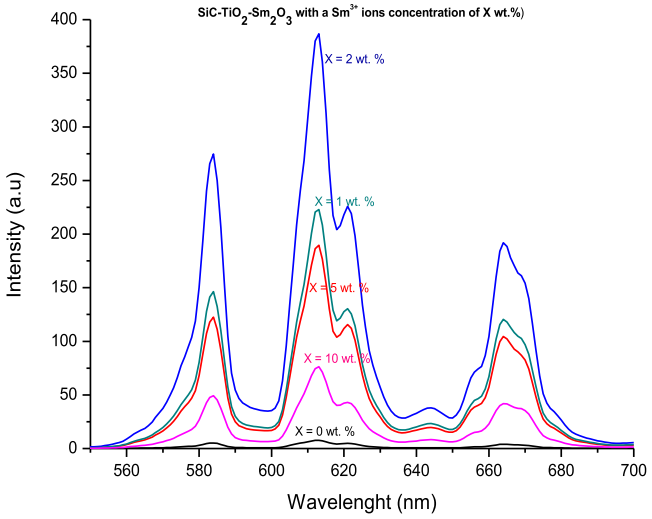

Figure 5. Emission spectra of SiC-TiO_2 and SiC-TiO_2-Sm_2O_3 powders with different Sm^{3+} ions concentrations: (a) 1.0 wt%, (b) 2.0 wt%, (c) 5.0 wt% and (d) 10 wt%, excited at 370 nm.

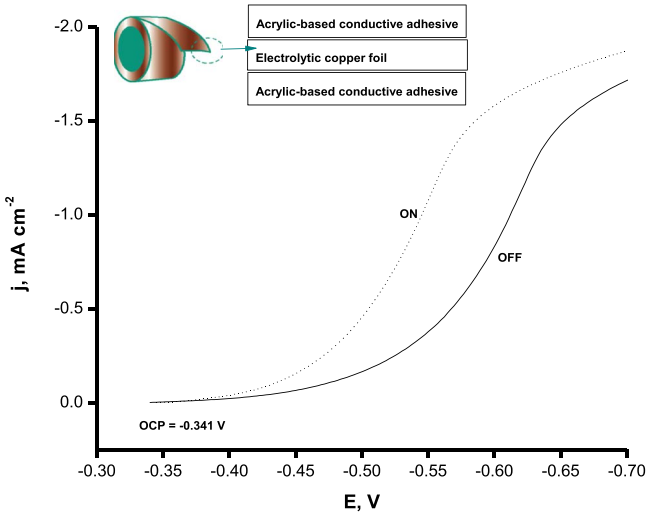

Figure 6. Linear voltammetry on adhesive copper tape (ACT) at a scan rate of 10 mV s^{-1} and under UV-light irradiation at 365 nm, (a) lamp turned off and (b) lamp turned on.

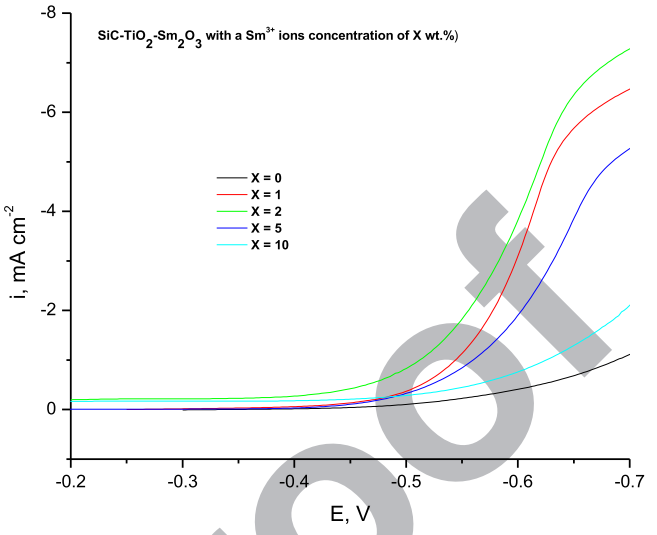

Figure 8. Linear voltammetry on SiC-TiO_2-Sm_2O_3 electrodes with different concentration of Sm^{3+} ions under dark conditions. Scan rate: 10 mV s^{-1}.

It is important to mention that the cathodic current recorded is associated to the hydrogen evolution reaction (HER) accordingly to the following equation:

$$2H^+ + 2e^- \rightarrow H_2 \quad [1]$$

Therefore the hydrogen is obtained as a result of the combination of electrochemical and photoelectrochemical processes; the increment of the cathodic current under light irradiation reveals the semiconductive nature of ACT substrate. The inset figure shows that the ACT is composed of two sides of acrylic-based conductive polymer.

The chemical stability of the ACT was evaluated using the infrared spectroscopy technique (FTIR). Figure 7 shows the spectra obtained on ACT before and after linear voltammetry test, where the absorption bands corresponding to the conductive polymer (adhesive) on the copper substrate are observed. The principal signals associated with ACT material are still appearing after fifth cycle of linear voltammetry, see Figure 7b. Although small changes in the absorption band at ca. 2958 cm^{-1} are observed, the electrochemical response is not modified;

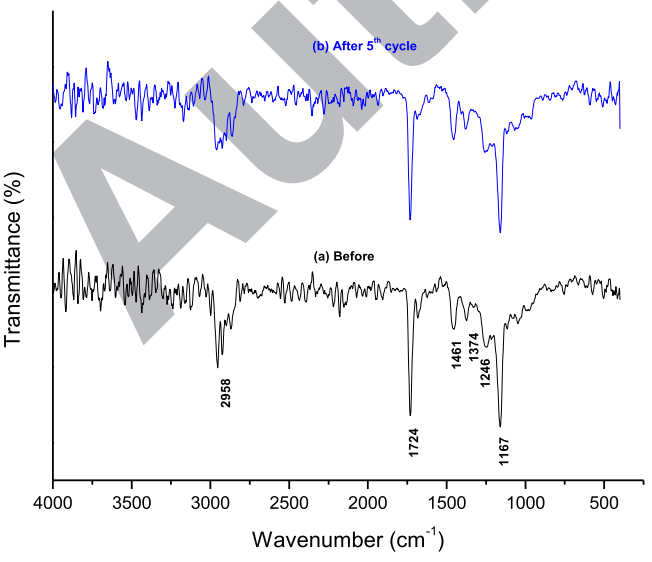

Figure 7. FTIR spectra obtained on ACT under two different conditions (a) before electrochemical experiment and (b) after 5th cycle of linear voltammetry in 0.5 M H_2SO_4 aqueous solution.

so this substrate can be used in the photoelectrochemical test of the ternary SiC-TiO_2-Sm_2O_3 system.

Electrochemical characterization of SiC-TiO_2-Sm_2O_3.—Figure 8 shows the linear voltammetry results of the prepared electrodes from the SiC-TiO_2-Sm_2O_3 mixture with different Sm^{3+} ions concentration. As it is known, the open circuit potential is a thermodynamic parameter that depends mainly on the interface between working electrode and the electrolytic solution.[48] Figure 8 shows that the value of E_{OCP} registered for each electrode depends on the samarium concentration. For all cases, the E_{OCP} value is more positive than that observed when the ACT was used as working electrode; this phenomenon is attributed to the formation of different electrode/solution interface in the electrochemical double layer. The value of E_{OCP} was monitored during a period of 30 minutes and it is remained practically constant, indicating mechanical and chemical stability in each SiC-TiO_2-Sm_2O_3 electrode.

In the Figure 8 it is also possible to detect that during the negative direction scan a negligible cathodic current is registered from E_{OCP} to −0.50 V, which indicates that no reaction is occurring in this potential range. For potential values lower than −0.50 V the cathodic current begins to take greater values, indicating that the HER is occurring in these applied potential values. Additionally, in Figure 8 it is clear to observe that the cathodic current intensity, associated to each SiC-TiO_2-Sm_2O_3 electrode, depends on the Sm^{3+} ions concentration in the compound. The values of the cathodic current are greater when Sm_2O_3 is incorporated in SiC-TiO_2. However, when the Sm^{3+} ions concentration is ca. 2.0 wt% the cathodic current intensity is the greatest and for concentration values >2.0 wt% the cathodic current value decreased.

The cathodic electric charges (Q_C) associated to the HER process were calculated from voltammograms in Figure 8 by numerical integration using the equation 2. The Q_C values for the SiC-TiO_2, SiC-TiO_2-Sm_2O_3 (1 wt%), SiC-TiO_2-Sm_2O_3 (2 wt%), SiC-TiO_2-Sm_2O_3 (5 wt%) and SiC-TiO_2-Sm_2O_3 (10 wt%) compounds were 0.1030, 0.6984, 0.9212, 0.4953 and 0.2655 mC cm^{-2}, respectively.

$$Q_C = \int_{OPC}^{-2V} \frac{i}{v} dE \quad [2]$$

The Q_C values are larger than that of unloaded SiC-TiO_2, where the maximum parameters (Q_C and i) at 2.0 wt% Sm^{3+} indicate that there is an optimal loaded concentration of Sm^{3+} ions in SiC-TiO_2-Sm_2O_3. This result indicates that activity which provokes a best activity of material for HER production.

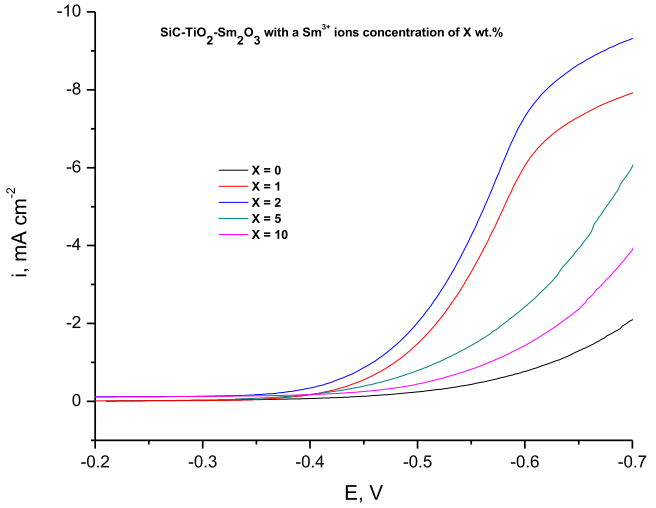

Figure 9. Linear voltammetry on SiC-TiO_2-Sm_2O_3 electrodes with different concentration of Sm^{3+} ions under UV-light irradiation conditions at 365 nm. Scan rate: 10 mV s^{-1}.

Photoelectrochemical characterization of SiC-TiO_2-Sm_2O_3.—The influence of the UV-light irradiation at 365 nm on SiC-TiO_2-Sm_2O_3 electrode was studied in the same potential range, E_{OCP} to −0.7 V and using the same aqueous solution. The comparison of the linear voltammograms obtained in these photoelectrochemical experiments is reported in Figure 9. The potential scan, which began in the negative direction, shows an increase in the cathodic current intensity after −0.4 V. The voltammetry response is mainly conditioned by the Sm_2O_3 content. In all cases, the values of cathodic photocurrent on SiC-TiO_2-Sm_2O_3 under UV light (Figure 9) are higher than those obtained for the same systems without light (Figure 8).

The calculation of cathodic charge associated with the process HER was carried out from equation 2. The cathodic charge values under UV light irradiation are 0.2019, 1.1628, 1.4515, 0.6106 and 0.4257 mC cm^{-2} for SiC-TiO_2, SiC-TiO_2-Sm_2O_3 (1.0 wt%), SiC-TiO_2-Sm_2O_3 (2.0 wt%), SiC-TiO_2-Sm_2O_3 (5.0 wt%) and SiC-TiO_2-Sm_2O_3 (10 wt%), respectively. These results indicate that the maximum value of Q_C at 2.0 wt% Sm_2O_3 occurred again. This behavior could be due to the efficient separation of photogenerated electron-hole pairs on SiC-TiO_2-Sm_2O_3 with 2.0 wt% Sm^{3+} ions concentration, as previously observed in photoluminescence results for this material.

In the literature[49] it is reported that when the concentration of metallic ions increases on the surface of materials, the surface barrier becomes high and the space charge region narrows, the electron-hole pair photogenerated within the region are efficiently separated by the large electric field before recombination. However, in this work we have detected that there is an optimal concentration of samarium, in which the system is more efficient (2.0 wt%). When the content of samarium is higher than the optimal concentration, the light captured by the SiC-TiO_2 diminishes due to the presence of Sm_2O_3 on its surface. Similar behavior has been mentioned in the literature for organic compounds degradation.[42,49] In the case of hydrogen production, Y. Zhang et al.[20] also reported a critical concentration of Cr_2O_3 to get the maximum activity of HER using the SiC-TiO_2 system.

Considering the characteristics of the lamp used in this experiment, it is possible to calculate the percentage of incident photon conversion efficiency (% IPCE) obtained for each photocathode (SiC-TiO_2-Sm_2O_3). The IPCE was calculated according to the following equation:

$$\%\text{IPCE} = \frac{1240 \times I_{PC}}{\lambda\,(\text{nm}) \times I_{INC}} \times 100 \qquad [3]$$

Where I_{INC} is the incident light power and I_{PC} is the photocurrent of the light irradiation at a specific wavelength (λ (nm)). In our case, the calculation of the cathodic photocurrent was obtained by the difference

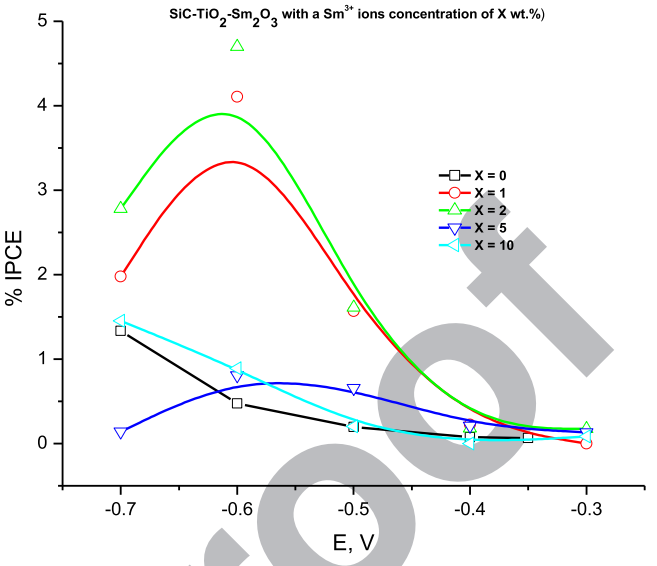

Figure 10. % IPCE of SiC-TiO_2-Sm_2O_3 with different concentration of Sm^{3+} ions: a) 0 wt%, b) 1.0 wt%, c) 2.0 wt%, d) 5.0 wt% and e) 10 wt%, under UV-light at 365 nm. The photocurrent was calculated from values of current in Figure 8 and 9 at the same potential.

between current value from photoelectrochemical and electrochemical processes, Figures 8 and 9, respectively.

Figure 10 shows that the %IPCE values are function of Sm_2O_3 concentration in SiC-TiO_2-Sm_2O_3 at different potential values. The maximum %IPCE value corresponds to the photocathode containing 2.0 wt% of Sm^{3+} ions concentration. These values were not corrected for electrolyte absorption and therefore must be considered as lower limits. The %IPCE values obtained are higher than those reported in the literature for similar systems of photoelectrochemical water splitting with %IPCE until 1%.[48] Therefore, the results here obtained indicate that the incorporation of an adequate amount of samarium in the SiC-TiO_2 compound improves the separation efficiency of the photogenerated electron-hole pairs, diminishing the electron-hole pair recombination rate and enhancing the photoelectrochemical water splitting activity.

Photoelectrochemical activity of the SiC-TiO_2-Sm_2O_3.— Figure 11 shows the current-time curves for the SiC-TiO_2-Sm_2O_3 electrodes with different Sm_2O_3 ion concentration under UV-light irradiation at

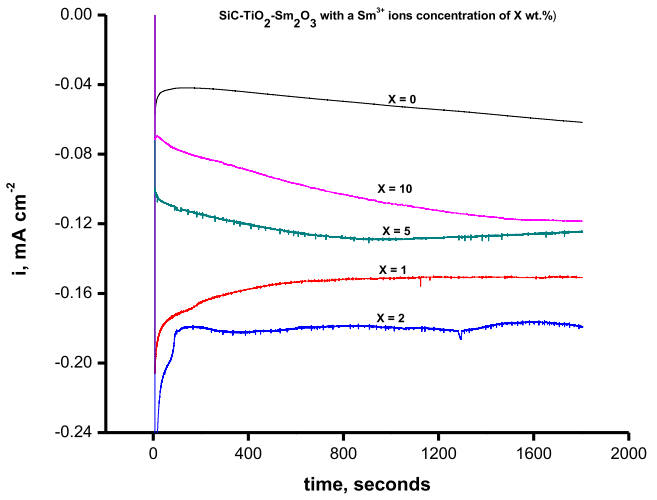

Figure 11. Current-time curves obtained from SiC-TiO_2-Sm_2O_3 with different concentration of Sm^{3+} ions: a) 0 wt%, b) 1.0 wt%, c) 2.0 wt%, d) 5.0 wt% and e) 10 wt%, under UV-light at 365 nm.

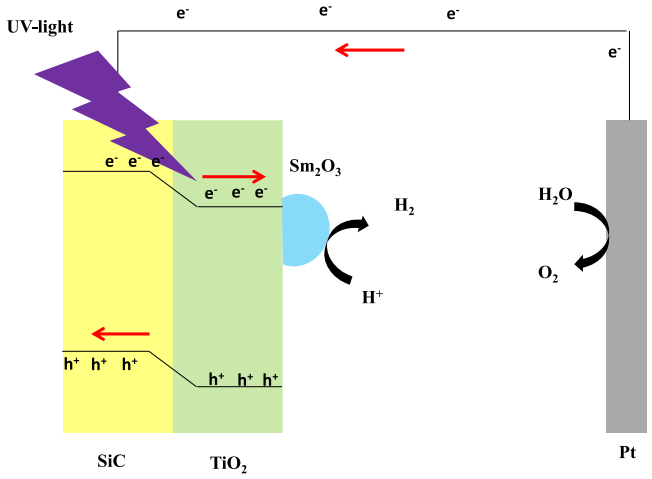

Figure 12. Scheme diagram of photoelectrochemical water splitting using SiC-TiO_2-Sm_2O_3 as electrode.

365 nm. The current transients were obtained at −0.5 V, during 1800 seconds in a 0.5 M H_2SO_4 solution. This potential value was chosen because the maximum %IPCE calculated value (see Figure 10) for all materials occurs at around −0.5 V.

The Figure 11 shows the cathodic current associated with the amount of hydrogen generated on the SiC-TiO_2-Sm_2O_3 photocatode under UV light during 1800 seconds. This figure indicates a negative current during all the photoelectrochemical experiments. This photo-induced cathodic current is obtained from the reduction of protons involving the photo-generation of electrons, and reveals the high activity of the SiC-TiO_2-Sm_2O_3 photoelectrode.[50] The cathodic current follows the same trend observed in the previous experiments by linear voltammetry.

Energy band diagram of the photoelectrochemical hydrogen production from SiC-TiO_2-Sm_2O_3.— The band positions of a semiconductor are very important to understand the photoelectrochemical performance. In this work, a synergy effect of SiC and TiO_2 semiconductors with the incorporation of Sm_2O_3 under UV-light radiation at 365 nm is occurring. When these materials are properly combined, a new way for the separation and charge transfer occurs. It is well known,[15] that SiC has a narrower bandgap than TiO_2. In the visible region the SiC produces excited electrons which flow to the TiO_2 and at the same time, holes of TiO_2 transfer back to SiC.

However, based on the results here presented, it is proposed that when the SiC-TiO_2-Sm_2O_3 material is under UV-light irradiation, the electron-hole pair separation is produced on both, SiC and TiO_2 semiconductors. Similar behavior has been reported by Y. Li et al.[15] for SiC-TiO-NiO composite, where NiO is loaded on TiO_2 surface and the excited electrons flow from TiO_2 to the NiO during the irradiation.

Finally, in this work the TiO_2-Sm_2O_3 acts as an electron collector where the hydrogen evolution occurs and SiC acts as a holes collector. In the case of SiC, it is considered as a p-type semiconductor and thus the holes generated in TiO_2 are transported to SiC. Therefore, samarium oxide can be considered as an electron collector in photoelectrochemical systems, which improves the hydrogen production in SiC-TiO_2 system. This mechanism is illustrated in Figure 12.

Conclusions

In this work, SiC-TiO_2-Sm_2O_3 was prepared by sol-gel method followed by thermal treatment with different content of samarium. Characterization of the synthesized SiC-TiO_2-Sm_2O_3 material by several techniques indicates that Sm^{3+} ions are as Sm_2O_3 and distributed on SiC-TiO_2 surface. SiC-TiO_2-Sm_2O_3 was used as an electrode in photoelectrochemical and electrochemical systems to generate hydrogen under application of a bias potential, E = −0.5 V. The produced photocurrent intensities are associated with the hydrogen production during the 1800 seconds of reaction and the results showed that the photocurrent value depends on the Sm_2O_3 amount in SiC-TiO_2-Sm_2O_3. Therefore it can be concluded that maximum hydrogen production occurred when samarium concentration in SiC-TiO_2-Sm_2O_3 is 2.0 wt%. Finally, the percentage of incident photon conversion efficiency was determined for each material and the results showed that this value increased as the samarium concentration increases, up to about 2.0 wt%, and then decreased abruptly.

Acknowledgments

Authors want to thank the financial support for this research to CONACYT through projects: FON.INST./75/2012 "Fotosíntesis Artificial," CNPq México-Brasil 2012-174247, REPAT-2012-191358 and CB-2011-168730, as well as PAICYT-UANL-2012.

References

1. W. C. Lattin and V. P. Utgikar. *Int. J. Hydrogen Energy* **32**, 3230 (2007).
2. H. Z. Wang, D. Y. C. Leung, M. K. H. Leung, and M. A. Ni. *Renewable and Sustainable Energy Reviews* **13**, 845 (2009).
3. R. Khotari, D. Buddhi, and R. L. Sawhney. *Renewable and Sustainable Energy Reviews* **12**, 553 (2008).
4. S. M. Kotay and D. Das. *Int. J. Hydrogen Energy* **33**, 258 (2008).
5. W. Balthasar and D. J. Hambleton. *Int. J. Hydrogen Energy* **5**, 21 (1980).
6. J. D. Holladay, J. Hu, D. L. King, and Y. Wang. *Catal. Today* **139**, 244 (2009).
7. T. A. Milne, C. C. Elam, and R. J. Evans. Report IEA/H2/TR-02/001, National Renewable Energy Laboratory, Golden, Colorado, 2002.
8. M. Ni, D. Y. C. Leung, M. K. H. Leung, and K. Sumathy. *Fuel Process. Technol.*, **87**, 461 (2006).
9. A. Fujishima, X. Zhang, and D. A. Tryk. *Int. J. Hydrogen Energy* **32**, 2664 (2007).
10. A. Fujishima and K. Honda. *Nature* **238**, 37 (1972).
11. T. Inoue and T. Yamase. *Chem. Lett.*, **14**, 869 (1985).
12. J. E. Turner, M. Hendewerk, and G. A. Somorjai. *Chem. Phys. Lett.*, **105**, 581 (1984).
13. S. Ida, Y. Yamada, T. Matsunaga, H. Hagiwara, T. Matsumoto, and Y. Ishihara. *J. Am. Chem. Soc.*, **132**, 17343 (2010).
14. S. Ida, K. Yamada, M. Matsuka, T. Matsunaga, H. Hagiwara, and Y. Ishihara, *Electrochim. Acta* **82**, 397 (2012).
15. Y. Li, Z. Yu, J. Meng, and Y. Li, *Int. J. Hydrogen Energy* **38**, 3898 (2013).
16. S. U. M. Khan, M. Al-Shahry, and W. B. Ingler, *Science* **297**, 2243 (2002).
17. J. H. Park, S. Kim, and A. J. Bard, *Nano Lett.*, **6**, 24 (2006).
18. S. K. Mohapatra, M. Misra, V. K. Mahajan, and K. S. Raja, *J. Phys. Chem. C* **111**, 8677 (2007).
19. C. C. Tsai and H. Teng. *Appl. Surf. Sci.*, **254**, 4912 (2008).
20. Y. Zhang, Y. Xu, T. Li, and Y. Wang. *Particuology* **10**, 46 (2012).
21. M. Ashokkumar. *Int. J. Hydrogen Energy* **23**, 427 (1998).
22. I. Lauermann and R. D. Memmingand Meissner. *J Electrochem. Soc.*, **144**, 73 (1997).
23. C. Schnabel, M. Worner, B. Gonzalez, I. Del Olmo, and A. M. Braun. *Electrochim. Acta* **47**, 719 (2001).
24. J. Akikusa and S. U. M. Khan. *Int. J. Hydrogen Energy* **27**, 863 (2002).
25. D. H. Van Dorp, N. Hijnen, M. Di Vece, and J. J. Kelly. *Angew. Chem. Int. Ed.* **48**, 6085 (2009).
26. N. Keller, V. Keller, F. Garin, and M. J. Ledoux. *Mater. Lett.*, **58**, 970 (2004).
27. S. Cerneaux, X. Xiong, G. P. Simon, Y. Cheng, and L. Spiccia. *Nanotechnology* **18**, 1 (2007).
28. H. Yamashita, Y. Nishida, S. Yuan, K. Mori, M. Narisawa, Y. Matsumura, T. Ohmichi, and I. Katayama. *Catal. Today* **120**, 163 (2007).
29. C. Gómez-Solís, I. Juárez-Ramírez, E. Moctezuma, and L. M. Torres-Martínez. *J. Hazardous Materials* **217**, 194 (2012). Q1
30. R. S. Pessoa, M. A. Fraga, L. V. M. Santos Massi, and H. S. Maciel. *Mat. Sci Semiconductor Processing* **29**, 56 (2015).
31. V. Keller and F. Garin. *Catal. Comm.*, **4**, 377 (2003).
32. I. Juárez-Ramírez, E. Moctezuma, L. M. Torres-Martínez, and C. Gómez-Solís. *Res. Chem. Intermed.*, **39**, 1523 (2013).
33. D. Hao, Z. Yang, C. Jiang, and J. Zhang. *Appl. Catal. B: Environ.*, **144**, 196 (2014).
34. T. H. Kim, C. Gómez-Solís, E. Moctezuma, and S. W. Lee. *Res. Chem. Intermed.*, **40**, 1595 (2014).
35. J. Oi-Uchisawa, A. Obuchi, R. Enomoto, J. Xu, T. Nanba, S. Liu, and S. Kushiyama. *Appl. Catal. B: Environ.*, **32**, 257 (2001).
36. A. J. Kenyon. *Progress in Quantum Electronics* **26**, 225 (2002).
37. J. H. Tao, J. Laski, N. Perea-Lopez, S. Shimizu, J. McKittrick, J. B. Talbot, K. C. Mishra, D. W. Hamby, M. Raukas, K. Klinedinst, and G. Hirata. *J. Electrochem. Soc.*, **56**, J158 (2009).
38. E. Millon, J. Perrière, S. Tricot, and C. Boulmer-Leborgne. *Proc. of SPIE* **7005**, 1A (2008).
39. T. Monteiro, A. J. Neves, M. C. Carmo, M. J. Soares, M. Peres, E. Alves, E. Rita, and U. Wahl. *Superlattices and Microstructures* **39**, 202 (2006).

40. R. P. Davies, C. R. Abernathy, S. J. Pearton, D. P. Norton, M. P. Ivill, and F. Ren. *Chem. Eng. Comm.*, **196**, 1030 (2009).
41. E. Guziewicz, B. A. Orlowski, B. J. Kowalski, I. A. Kowalik, A. Reszka, L. Wachnicki, S. Gieraltowska, M. Godlewski, and R. L. Johnson. *Appl. Surf. Sci.*, **282**, 326 (2013).
42. Y. Wang, H. Cheng, L. Zhang, Y. Hao, J. Ma, B. Xu, and W. Li. *J. Mol. Catal. A: Chem.*, **151**, 205 (2000).
43. L. M. Torres-Martínez, R. Gómez, O. Vázquez-Cuchillo, I. Juárez-Ramírez, A. Cruz-López, and F. J. Alejandre-Sandoval. *Catal. Comm.*, **12**, 268 (2010).
44. Y. Li, G. Wang, L. Meng, Y. Zhao, B. Jiang, S. Liu, B. Xu, Y. Wang, and J. Su. *Mat. Res. Bull.*, **50**, 203 (2014).
45. Y. Tian, Y. Liu, R. Hua, L. Na, and B. Chen. *Mat. Res. Bull.*, **47**, 59 (2012).
46. V. A. Zeitler and C. A. Brown. *J. Phys. Chem.*, **61**, 1174 (1957).
47. X. L. Wang, B. Yan, and J. L. Liu. *Photochem. Photobiol. Sci.*, **10**, 580 (2011).
48. Southampton Electrochemistry Group, *Instrumental Methods Electrochemistry*, Ellis Horwood Limited, England, 1985.
49. R. Van de Krol and M. Grätzel, *Electronic Materials: Science & Technology*, Editorial Springer, USA, 2012.
50. Y. K. Hsu, C. H. Yu, Y. C. Chen, and Y. G. Lin. *Electrochim. Acta* **105**, 62 (2013).

Query

Q1: AU: Please provide a digital object identifier (doi) for Ref(s) 29. For additional information on doi's please select this link: http://www.doi.org/. If a doi is not available, no other information is needed from you.